Long-Term Experimental Campaign on RC Shrinkage Cracking: Conceptualization, Planning and Experimental Procedures

José Gomes, José Granja, Carlos Sousa, Cláudio Ferreira, Dirk Schlicke, Rui Faria, and Miguel Azenha

Abstract Numerical and analytical simulation of cracking in reinforced concrete (RC) structures requires laboratory testing for validation of assumptions and calibration of modelling strategies. The scale, complexity and innovation of these experiments can present a challenge, even for experienced professionals, and a significant amount of time, effort and money might be inadequately invested on unsuitable test setups, or poorly planned experimental campaigns. This paper deals with the lessons learned from a complex long-term experimental campaign on RC slabs subjected to flexural cracking and restrained shrinkage. It intends to serve as a steppingstone for future works of the same nature. The final version of the restraining device is described and decisions on tested specimens, test conditions, sensing and material characterization are explained based on the available resources. The most relevant tasks during preparation of the long-term experimental campaign are described in detail. Finally, the hard-ships and problems faced during implementation of the experimental program, and the way they were overcome, are addressed. The application of concepts in line with Building Information Modelling (BIM) methodologies, such as object-oriented modelling and process maps, for design of the test setup and task scheduling, was of crucial importance for the success of the experimental campaign.

Keywords Service life behaviour · Experimental testing · Restrained shrinkage · BIM · Reinforced concrete slabs

J. Gomes · J. Granja · M. Azenha (✉)
School of Engineering, University of Minho, Guimarães, Portugal
e-mail: miguel.azenha@civil.uminho.pt

C. Sousa · C. Ferreira · R. Faria
Faculty of Engineering, University of Porto, Porto, Portugal

D. Schlicke
Graz University of Technology, Graz, Austria

F. Kanavaris et al. (eds.), *International RILEM Conference on Early-Age and Long-Term Cracking in RC Structures*, RILEM Bookseries 31,
https://doi.org/10.1007/978-3-030-72921-9_12

1 Introduction

One of the main features of concrete that designers have to deal with is the time-dependent nature of its behaviour. This can either have an adverse effect on the structural performance (e.g., when self-induced stresses or loss of prestressing are caused by restrained shrinkage or creep effects, respectively), or a beneficial effect when stresses are redistributed or decreased due to creep [1, 2]. The study of interactions that occur in the context of the aforementioned time-dependent properties in the process of crack development is of paramount importance to provide better methodologies for crack width prediction in RC structures.

The main challenge in studies of this nature is the experimental validation of assumptions and models. In that regard, several experimental studies on this subject have been performed over the last years. Gilbert and Nejadi [3] performed an experimental campaign of long-term tests on RC beams and slabs in order to assess the effect of internal restraint on crack development. Different Variable Restraint Frame (VRF) testing systems, which enable the testing of restrained RC ties, have been proposed by Cusson and Hoogeven [4], Faria et al. [5] and Schlicke et al. [6]. More recently, Gomes et al. [7, 8] proposed a test setup for simultaneous application of axial restraint and vertical loads in slab-like specimens. By providing information that is complementary to [8], this paper describes in detail the conceptualization, planning and experimental procedure of the latter, which was performed by this research team, and it is aimed to be a guideline for future experimental programs of the same nature.

Section 2 reports the development of the experimental setup, devised to axially restrain a slab-like specimen subjected to vertical loading, while in Sect. 3 the preparation and conduction of the experimental program is addressed.

2 Description of the Restraining Device

2.1 Overview

The main requirement of the restraining device is the ability to provide a controlled axial restraint level to a pre-defined control region of a slab-like test specimen, while simultaneously allowing it to endure bending and shear stresses. The underlying operating principle can be explained with support of Fig. 1. It relies on a simply supported RC specimen (thus representing the region of positive bending moments of a real continuous slab) in which the supports are embedded at mid-height (and shrouded by the longitudinal reinforcement), and the longitudinal displacement of one of the supports is controlled by the user with a hydraulic driven force. Even though detailed information on sizing and requirements can be found in [7], they are generally addressed in the following paragraphs.

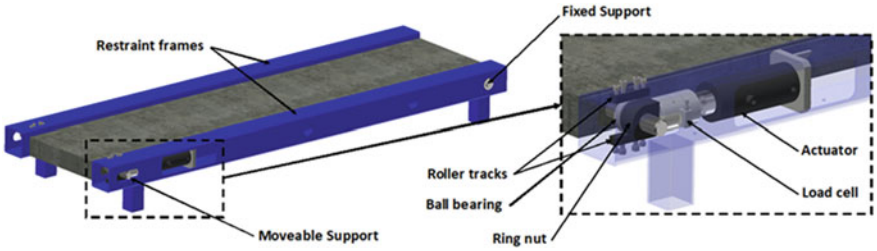

Fig. 1 Schematic view of the restraining device

The design of the test specimens is based on a continuous solid slab supported by transverse beams at every 4 m. The slab was designed for the ultimate limit state, considering permanent loads of 2.0 kN/m^2 (besides self-weight) and live loads of 3.2 kN/m^2. Such approach resulted in a 0.10 m thick slab (C20/25), longitudinally reinforced for bending with ϕ8//0.10 (S400C) and with a secondary transverse reinforcement of ϕ6//0.25, providing adequate service life behaviour without consideration of the effects of axial restraint (which was considered a design starting point).

The design of the restraining device was performed by taking into account the following assumptions: (i) the test specimen is 2.6 m long, with a free span of 2.4 m to match the distance between zero bending moments of the slab (~3/5 of the slab's effective span); (ii) the cross section of the test specimen is 0.1 × 0.5 m^2 to ensure a width-to-depth ratio of 1/5 and, consequently, a slab-type behaviour; (iii) even though the test specimen is subjected to positive bending moments only, no reinforcement curtailment is considered, and the same reinforcement is attributed to the top and bottom layers (for simplification of execution and analysis); (iv) the test specimen will not endure restraining forces higher than concrete's axial cracking force $N_{cr} = A_c \times f_{ctm}$.

The restraining device consists of two reaction frames supporting the test specimen, each one housing a hydraulic actuator and a load cell connected to one of the supports. The test specimen is supported by two solid steel rods, with a diameter of 40 mm, embedded at mid-height. One steel rod—the fixed support—is inserted in the 40 mm holes located in the lateral side of the reaction frames; the other steel rod—the moveable support—is inserted in the ring nuts (connecting the support to the load cells and actuators) and in the radial ball bearings (which carries the vertical load). The radial ball bearing is located between two roller tracks whose position is adjusted with 4 socket head cap screws, being relieved from top roller track immediately after casting to enable longitudinal sliding. The axial restraint of the test specimen is performed with the two double effect hydraulic actuators (with a 100 kN capacity in compression, each), connected in parallel to a manual hydraulic pump. The axial load applied to the test specimen is monitored with two resistive load cells (measurement range of 100 kN, each), positioned between the actuator and the ring nut.

2.2 *Object Oriented Modelling of the Restraining Device*

Given the complexity of the devised test setup, with several elements of different nature interacting with each other, the modelling of the restraining device was performed with an object-oriented approach, in which the model is composed by objects that, besides the geometric parameters, are attributed with other type of data (e.g., information about manufacturer, cost and technical features) and procedures (namely spatial relations with adjacent objects and behaviour rules). Such approach enables the development of complex models in periods of time that would not be possible with conventional computed aided design (CAD) software, and reduces the risk of mistakes through automatic detection of incompatibilities.

The model for the restraining device was developed in AutoDesk Inventor Professional 2018. It is composed by several assemblies, which includes the steel components of the reaction frames and support system, actuators and load cells, wood components for formwork and propping system, and the test specimen. Figure 2 shows an exploded view of the restraining device and subsequent stages of the test setup assembly, automatically generated from the final model.

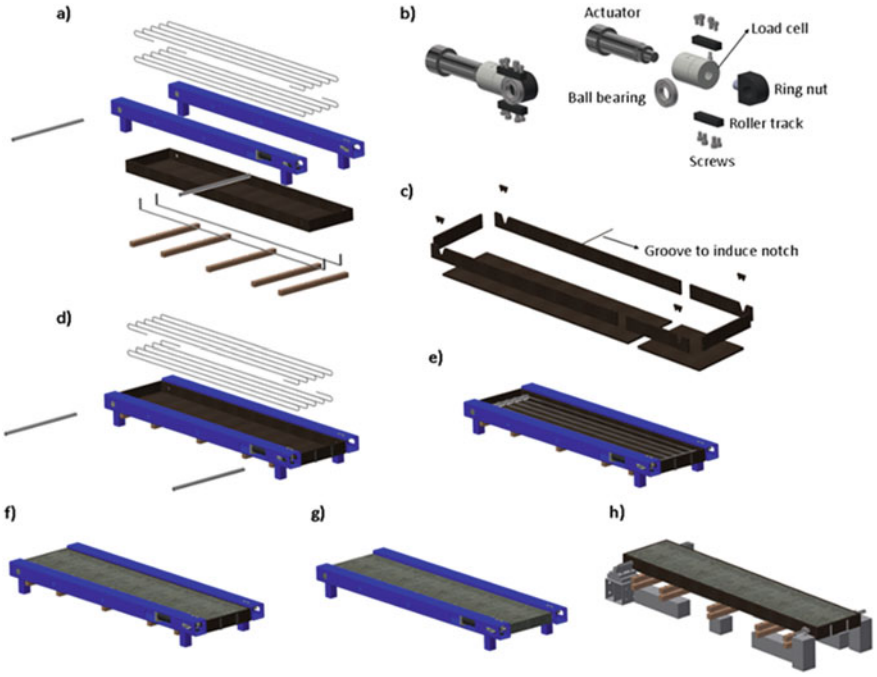

Fig. 2 Exploded view of test setup: **a** pre-assembled restraining system; **b** components inside the restraint frame; **c** pre-assembled formwork; **d** positioning and propping of formwork; **e** positioning of longitudinal rebars and steel rods; **f** casted test specimen; **g** test specimen after formwork removal; **h** support and formwork propping systems for unrestrained specimen

The STP file format for interoperability of the general industry [9] was used to order the production of these components, allowing for a straightforward process. The model contains information regarding the geometry of the different components and the spatial relation between them, as well as material information and object standardized references. The components inside the restraint frame, presented in Fig. 2b (assembled and isolated), were defined based on the requirements described in Sect. 2.1; specific information regarding the brand and commercial references was also included in the model. For the remaining components, only information about the material was attributed, besides the geometry and spatial relation with other components.

The formwork was designed to facilitate its extraction from the climatic chamber and to avoid damaging the test specimens during its removal. It is divided longitudinally into two parts (connected by two metallic plates with a 5×20 mm^2 cross-section), and it is composed by eight 18 mm thick plywood panels, connected with metallic L-shaped brackets screwed to the bottom and lateral sides (Fig. 2c). A PVC groove with triangular cross-section (13 mm wide and 8 mm deep) is glued to the bottom of the formwork, to induce a notch on the test specimen and consequent cracking at mid-span. After the formwork is assembled, it is positioned and fixed through five timber slats bolted to the bottom face of the restraint frames (Fig. 2d). The longitudinal rebars are then duly positioned inside the formwork. The notches on the lateral panels of the latter enable the insertion of the steel rods, as described in Sect. 2.1, through the reinforcement, between top and bottom rebars (Fig. 2e). The negative of the notch that is not filled by the supporting rod is sticked to the formwork with insulating tape. The position of the moveable support is adjusted and fixed with the roller tracks and head cap screws before casting the specimen. Immediately after casting (Fig. 2f), the top roller tracking is relieved to enable longitudinal displacement. After the curing period, the formwork is removed by unscrewing the metallic plates and L-shapes, as well as the timber slats (Fig. 2g). Alternative support and formwork propping systems were devised to account for simultaneous testing of unrestrained specimens under similar conditions (Fig. 2h).

3 Long-Term Experimental Campaign

3.1 Experimental Strategy

In order to address the effects of both degree of restraint and level of flexural loading, the experimental campaign involved the simultaneous testing of four distinct situations, as presented in Fig. 3. Two test specimens were subjected to external axial restraint and different levels of vertical load: SLAB1 was submitted to the quasi-permanent load combination, while SLAB2 was merely subjected to its self-weight. One test specimen, SLAB3, was subjected to the same vertical loading as SLAB1, but without any external axial restraint. A fourth situation, with no restraint forces

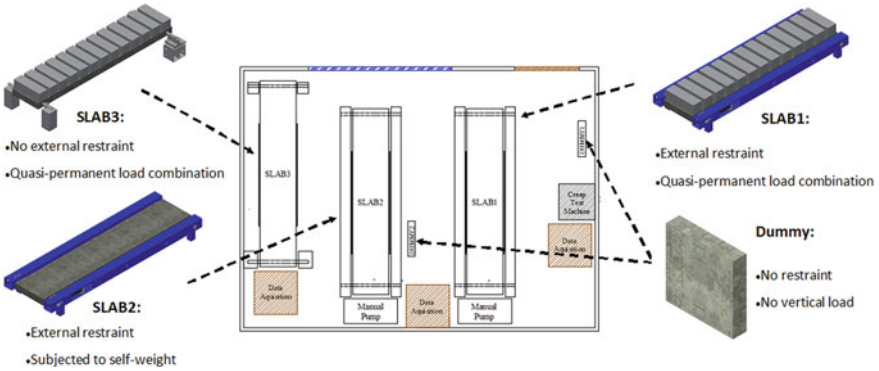

Fig. 3 Arrangement of test specimens in the climatic chamber

nor vertical loading (allowing to determine the imposed deformation that former slabs are subjected to) was simulated with two dummy specimens, DUMMY1 and DUMMY2, with the same cross section and subjected to the same drying history as former slabs, 0.5 m long (positioned vertically) and with no reinforcement.

The experimental program was conducted over a period of 18 months, in a climatic chamber with constant environmental conditions (T = 20 °C and RH = 60%). It was complemented with companion specimens for measurement of RH profiles and characterization of the following concrete properties, at different ages: compressive strength, tensile strength, E-modulus and creep in compression.

The structural behaviour of the test specimens was assessed, during the entire experimental campaign, with continuous monitoring of vertical displacements at mid-span, average in-plane deformations in the control region, steel strains at both top and bottom reinforcement and crack width development.

3.2 Preparation of the Experimental Campaign

The preparation for the long-term experimental campaign involved several tasks at different stages: it included minor enhancements to the test setup based on the pilot test outcomes, the construction of a large-scale climatic chamber, instrumentation of test specimens and elaboration of a micromanagement plan for casting day.

In order to increase efficiency and minimize errors, these tasks were carefully planned with process maps, in which both structured workflows for predicted scenarios and protocols to respond to dynamic situations were considered. A process map visually shows, through different flowcharts shapes, the steps of a work activity, the actors that are involved in carrying out those activities and information flows between them. The standard Business Process Model and Notation (BPMN), developed by the Object Management Group (OMG), is often used to create process

maps, as it provides a notation that is readily understandable by all users and creates a standardized bridge between process design and process implementation [10].

The most relevant preparation activities will be addressed in the following subsections, apart from the pilot test, whose detailed description can be found elsewhere [7] and will not be discussed here for the sake of brevity.

Construction of climatic chamber. The climatic chamber, depicted in Fig. 4, was specifically constructed for this experimental campaign to eliminate the influence of temperature and ambient RH variations in the results, thus simplifying the analysis. Given the large area that was needed to include all test specimens, as well as the available funds for the project, the following cost-efficient solution was envisaged: a room with a net area of 3.6×4.9 m^2, built with double layer wood panels and 5 cm thick XPS modules. A moveable roof made of a sandwich panel was considered to enable the removal of test specimens at the end of the experimental campaign, thus allowing it to be reused for other projects. The environmental conditions were kept constant with an air conditioning device, a humidifier and a dehumidifier working simultaneously. This solution provided a test room with constant T and RH of 20 °C $\pm$ 0.5 °C and 60% $\pm$ 5%, respectively. A restricted access policy was implemented to avoid unnecessary entrances from people outside the research group, and a double layer laminated glass (2.0×2.1 m^2) allowed to visualize the test setup from outside. These measures minimized environmental contamination and human-caused technical issues.

Instrumentation and setup of the longitudinal strain measurement system. For assessment of the structural behaviour of the test specimens, the following sensors were used: (i) vibrating wire strain gauges for measurement of dummy specimens' deformations; (ii) electrical resistance strain gauges and optical fibre Bragg grating sensors for measurement of strains in the longitudinal rebars; (iii) hand-held USB microscope for measurement of crack widths; (iv) thermo-resistance PT100 for measurement of the temperature inside the test specimens and (v) linear variable differential transducers (LVDTs) for measurement of deflections and longitudinal average strains in the control region. The following paragraphs describe the devised measurement system for assessment of the longitudinal strains in the control region, which was gradually improved until the presented final version. Detailed information regarding the remaining measurement devices can be found elsewhere [8].

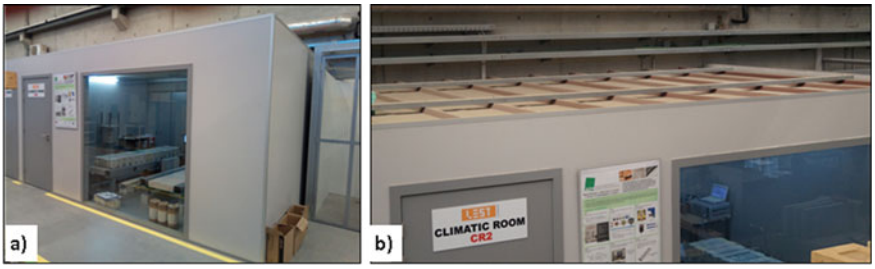

Fig. 4 Climatic chamber: **a** view from the outside; **b** roof detail

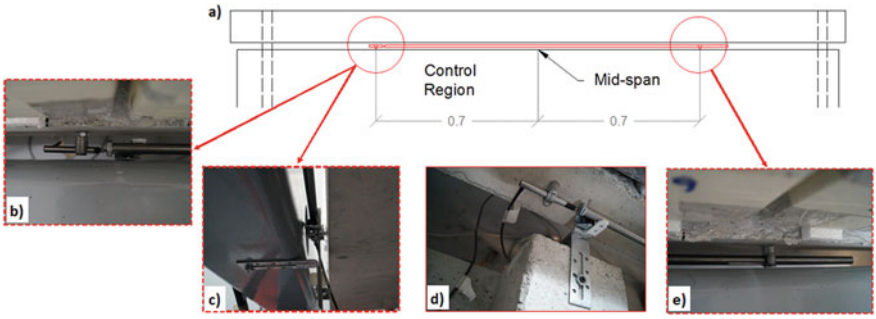

Fig. 5 Longitudinal strains measurement system (final version): **a** outline; **b** detail of LVDT; **c** detail of roller support; **d** setup for unrestrained specimen; **e** fixed extremity

After application of the restraint load, significant cracking was expected at both extremities due to stress concentration near the steel rods. For that reason, the measurement of the average axial strains (for control of the restraining condition) was limited to the 1.4 m long central region. For assessment of the longitudinal strains in this control region, a measurement system with one LVDT on each side of the test specimen was used, as illustrated in Fig. 5.

For installation of this measurement system, two hexagonal nuts M6 were pre-embedded on each lateral side of the test specimens, at mid-height and spaced 0.7 m from the mid-span. The average longitudinal deformation was measured with one LVDT on each side of the slab, fixed to a metallic clamp screwed to the pre-embedded nut on one extremity and in contact with a 12 mm diameter steel tube, which was fixed to a metallic clamp screwed to the other extremity. Near the point of contact between the LVDT and the steel tube, the latter was supported by a roller fixed to the metallic frame of the restraint device (SLAB1 and SLAB2) or to a concrete block (SLAB3).

Micromanagement plan for the casting day. Considering the limited space inside the climatic chamber, the number of sensors installed and the number of concrete specimens for testing and material characterization, a micromanagement plan for the casting day was developed to ensure that all test specimens were cast in a small-time period, during which the fresh concrete age can be considered the same. It is worth mentioning that, due to its complexity, the development of a dedicated process map [11] for this activity, which involved 14 people from the research team, was of paramount importance for its success. The roles of each person during this task, and the interaction between them, are described in detail in the next paragraphs and schematized in Fig. 6.

Persons identified with the numbered circles 01–05 were responsible for casting the test and dummy specimens. Two vibrating needles were available inside the climatic chamber to be used by persons 01 and 02, which were responsible for vibrating the concrete. Persons 03–05 were responsible for filling the formworks with concrete buckets. The interchange of the concrete buckets between inside and outside the climatic chamber was assured by persons 06 and 07, while persons 08–10 were

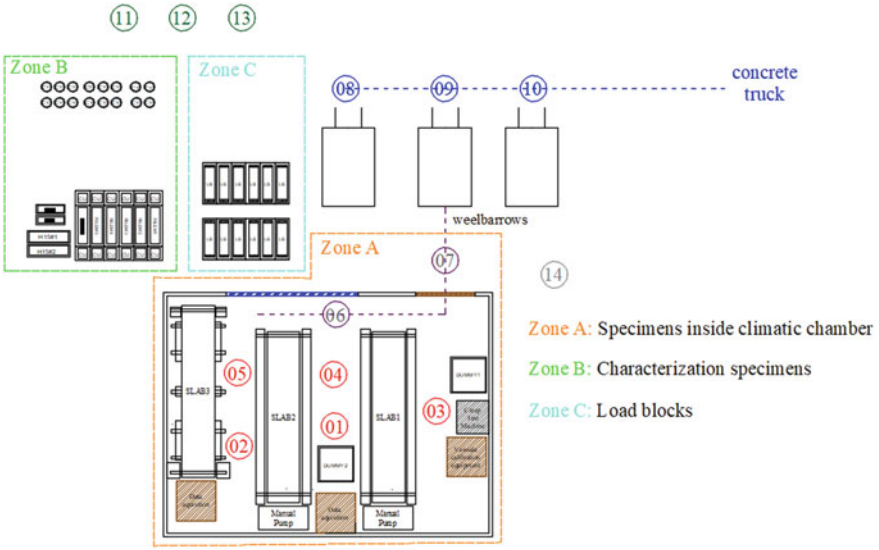

Fig. 6 Micromanagement plan for the casting day

responsible for the transportation of concrete on wheelbarrows from the concrete truck and for filling the empty buckets. The specimens for concrete characterization and load blocks were cast outside the climatic chamber by persons 11–13. Person 11 was in charge of vibrating the concrete with a vibrating needle, and persons 12–13 of filling the moulds with concrete buckets. Person 14 was responsible for the photographic recording of the casting (Fig. 7).

Right after casting, all specimens were duly sealed with plastic film, and characterization specimens were taken to the climatic chamber. The casting took place on April 17, 2018, mixing of concrete started at 13:54 and the concrete truck arrived at the casting site at 14:35. A slump test was performed to check the consistency class (120 mm slump—class S3). The casting of the test specimens started at 14:50 and ended at 15:40.

3.3 Experimental Campaign and Control of Restraining Condition

The test specimens were left undisturbed until formwork removal. After a curing period of 7 days, all test specimens were carefully demoulded and exposed to the climatic chamber environment. The formwork was gradually removed by unscrewing the metallic L-shaped brackets first (to reduce friction between concrete and formwork), and then removing the timber slats. During this process, 3 LVDTs

Fig. 7 Casting of the long-term experimental campaign: **a** arrival of concrete truck; **b** filling the wheelbarrows; **c** transportation of concrete buckets; **d** casing the slab specimens; **e** vibrating slab specimens; **f** casting load blocks and characterization specimens; **g** vibrating load blocks and characterization specimens; **h** sealing the test specimens; **i** sealing the characterization specimens

were positioned on the top surfaces, at mid-span, to measure the vertical deflection (Fig. 8a).

The formwork removal was immediately followed by installation of LVDTs for measurement of vertical displacements, as well as the lateral measurement system for assessment of the longitudinal strains in the control region. Early measurements of longitudinal deformations in the control region showed that the devised measuring system was being affected by friction effects (recorded deformations developed in steps, instead of showing a continuous variation). Even though this issue was mitigated at 22 days of age, by reducing the distance between the measurement system and the lateral side of the slab (final form is presented in Fig. 5), the initial intent of providing full compensation of the average longitudinal strain in the control region by adapting the axial force, was withdrawn. Instead, the restraining procedure for SLAB1 and SLAB2 was performed by controlling an expected restraint force throughout time. The expected restraint force was estimated before each increment of axial load by performing viscoelastic analyses based on the age-adjusted elastic modulus (AAEM) method [12] and experimental measurements of free shrinkage and crack width: the AAEM method was applied to determine the axial load increment needed to fully compensate the longitudinal deformation, considering the recorded free shrinkage strains, while the recorded crack widths were used to update the average deformation in the cracked zone.

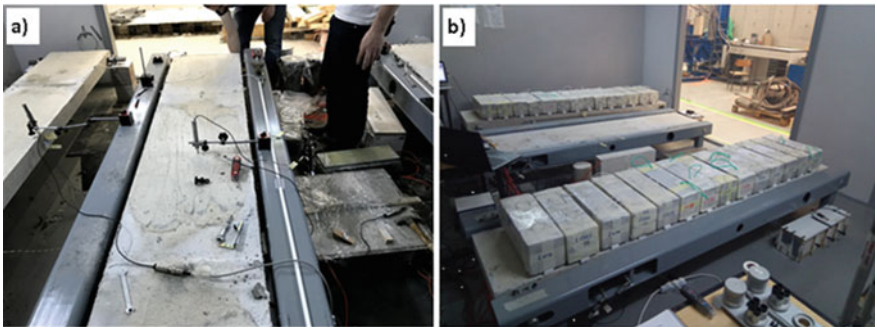

Fig. 8 Key instants of long-term experimental campaign: **a** formwork removal; **b** application of vertical loads

At the age of 50 days, SLAB1 and SLAB3 were subjected to a distributed load of 2.96 kN/m^2. In a passive restraint system, the imposition of external bending may result in the decrease of the axial restraint force due to widening and formation of cracks [13, 14]. However, the devised restraint system was not under closed loop displacement control (the restraint force depends on the oil pressure in the hydraulic actuators), and the restraint force decrease had to be estimated (using the AAEM method) and applied manually in SLAB1, over 4 stages. At each stage, the load blocks were strategically placed to induce ~25% of the final bending moment increment, followed by a reduction of ~25% of the calculated restraint force decrease. It is worth noting that the load blocks were adequately separated from each other (thus avoiding significant arch effects), and supported by $20 \times 40 \times 480$ mm^3 XPS stripes to enable concrete drying from the slabs' top surface (Fig. 8b).

At the end of the fourth stage, it was observed that the calculated restraint force decrease was overestimated (no new cracks were formed), and the axial load in SLAB1 was progressively increased until a situation of near full restraint (measured longitudinal strain in the control region close to 0 μm/m). From 60 days onwards, the axial force on both SLAB1 and SLAB2 was kept constant.

The presentation and analysis of the results obtained in this experimental campaign are out of the scope of this paper and can be found elsewere [8].

4 Conclusions

This paper deals with the preparation and conduction of a long-term experimental campaign on slabs subjected to restraining shrinkage and vertical loads, with special focus on design and planning approaches. The following conclusions are drawn.

The restraining device proposed in this work was capable of imposing and controlling a pre-defined level of axial load on the test specimens, while allowing them to endure shear and bending stresses. The object-oriented modelling approach allowed

to develop the test setup without the need of substantial corrections after deployment of a pilot test.

The use of process maps at micromanagement level was of paramount importance for the successful casting of several test specimens, highly instrumented, in a very confined space, in a short period of time and without equipment failure.

Initial difficulties regarding the measurement system for longitudinal strains in the control region were overcome with an alternative plan to restrain the test specimens, based on different measurement procedures. Even though those measurements were not meant for redundancy, it shows the importance of having a wide range of measurement systems in large scale experiments.

Acknowledgements Funding provided by the Portuguese Foundation for Science and Technology (FCT) to the Research Project IntegraCrete (PTDC/ECM-EST/1056/2014 POCI-01–0145-FEDER-016841) and to the PhD Grant SFRH/BD/148558/2019 is acknowledged. This work was also financially supported by UIDB/04029/2020—ISISE and by UIDB/04708/2020—CONSTRUCT, funded by national funds through the FCTMCTES (PIDDAC). The authors also acknowledge the contribution of Ali Edalat-Behbahani, Amin Abrishambaf, António Matos, César Gonçalves, Fernando Pokke, José Ferreira, Marco Jorge, Meera Ramesh, Ricardo Cruz, Sérgio Soares and Sónia Soares during the casting of the experimental campaign.

References

1. Azenha, M.: Numerical simulation of the structural behaviour of concrete since early ages. Ph.D. Thesis, University of Porto, FEUP (2009)
2. Leitão, L.: Análise termo-higro-mecânica das tensões autoinduzidas em estruturas de betão. Ph.D. Thesis, University of Porto, FEUP (2018)
3. Gilbert, R.I., Nejadi, S.: An experimental study of flexural cracking in reinforced concrete members under sustained loads. In: UNICIV Report. School of Civil & Env. Eng., Sydney (2004)
4. Cusson, D., Hoogeveen, T.: An experimental approach for the analysis of early-age behaviour of high-performance concrete structures under restrained shrinkage. Cem. Concr. Res. **37**(2), 200–209 (2007)
5. Faria, R., Leitão, L., Teixeira, L., Azenha, M., Cusson, D.: A structural experimental technique to characterize the viscoelastic behavior of concrete under restrained deformations. Strain **53**(1) (2017)
6. Schlicke, D., Hofer, K., Tue, N.V.: Adjustable restraining frames for systematic investigation of cracking risk and crack formation in reinforced concrete under restrained conditions. In: Serdar, M., et al. (eds.) Advanced Techniques for Testing of Cement-Based Materials, pp. 211–239. Springer International Publishing (2020)
7. Gomes, J., Azenha, M., Granja, J., Faria, R., Sousa, C., Zahabizadeh, B., Edalat-Behbahani, A., Schlicke, D.: Proposal of a test set up for simultaneous application of axial restraint and vertical loads to slab-like specimens: sizing principles and application. In: SynerCrete'18: Interdisciplinary Approaches for Cement-Based Materials and Structural Concrete: Synergizing Expertise and Bridging Scales of Space and Time, RILEM, Funchal, Madeira Island (2018)
8. Gomes, J.G., Granja, J., Sousa, C., Zahabizadeh, B., Faria, R., Schlicke, D., Azenha, M.: A new test setup for simulation of the combined effect of bending and axial restraint in slab-like specimens. Eng. Struct. **225** (2020)

9. ISO: ISO 10303: Industrial automation systems and integration—product data representation and exchange (1994)
10. OMG: Business Process Model and Notation (BPMN). In. Edited by (OMG) OMG (2013)
11. Gomes, J., Azenha, M.: Process map for casting a long-term experimental campaign on RC shrinkage cracking. Dataset (2021). https://doi.org/10.5281/zenodo.4474539
12. Bazant, Z.P.: Prediction of concrete creep effects using age-adjusted effective. J. Am. Concr. Inst. **69**(4), 212–217 (1972)
13. Camara, J., Luís, R.: Structural response and design criteria for imposed deformations superimposed to vertical loads. In: The Second fib Congress: 2006, Naples, Italy, pp. 1–12 (2006)
14. Gomes, J., Carvalho, R., Sousa, C., Granja, J., Faria, R., Schlicke, D., Azenha, M.: 3D numerical simulation of the cracking behaviour of a RC one-way slab under the combined effect of thermal, shrinkage and external loads. Eng. Struct. **212** (2020)